Lipid Vesicle Fusion as a Vehicle to Study Transmembrane Protein Interactions

---

A Dissertation

Presented to

The Doctoral Program Committee

At the University of Missouri-Columbia

In Partial Fulfillment

Of the Requirements for the Degree

Doctor of Philosophy

By

Bryan M. Lada

Dr. Kent Gates, Dissertation Supervisor

July 2021

The undersigned, appointed by the dean of the Graduate School,

have examined the dissertation entitled

Presented by Bryan M. Lada

a candidate for the degree of doctor of philosophy,

and hereby certify that, in their opinion, it is worthy of acceptance.

Professor Kent Gates

Professor C. Michael Greenlief

Professor Gary Baker

Professor Peter Cornish

Acknowledgements

I would first like to thank my committee, Drs. Kent Gates, C. Michael Greenlief, Gary Baker and Peter Cornish. I could not have done it without their extreme, unwavering patience, guidance, insights, mentorship, and never-ending support to help see me through the journey.

Thanks to Drs. Jason Cooley and Renee Jiji and their respective research groups and the Baker research group. Thanks to the University of Missouri-Columbia and the Chemistry Department for the space to conduct this work in addition to the financial support.

Special thanks to Drs. Michael Eagleburger, Teng-Wei Wang, Anahita Zare, Mia Brown, and Nate Larm for all the support, the laughs, their guidance and above all else their friendship.

Finally, and most importantly, thanks to my family. Thanks to my parents, Mary & Raymond Russo and Edward Lada, my aunt, Debra Lada, my sisters Megan Houlihan and Karen Lentz for their unending love, support, and patience from start to finish.

A special dedication to my grandparents, Daniel Barciszewski, Mary Lou Lada, and Delma Russo. I wish they could have been here to see it.

M-I-Z!!!

Table of Contents

List of Figures and Tables

Abbreviations

Aβ	Amyloid Beta
ACN	Acetonitrile
ANTS	8-aminonapthalene 1,3,6-trisulfonic acid
APP	Amyloid Beta Precursor Protein
CD	Circular Dichroism
CPB	Citrate-Phosphate Buffer
DG 12:0	1,2-dilauroyl-sn-glycerol

DLEPC

- 12:0 EPC – 1,2-dilauroyl-sn-glycero-3-ethylphocholine
- 14:0 EPC – 1,2-dimyristoyl-sn-glycero-3-ethylphocholine
- 16:0 EPC – 1,2-dipalmitoyl-sn-glycero-3-ethylphocholine

DLPC	1,2-diauroyl-sn-glycero-3-phosphocholine
DLPG	1,2-diaurroyl-sn-glycero-3-phospho-(1-rac-glycerol)
DLS	Dynamic Light Scattering
DPX	p-xylene-bis-pyridiumbromide
dUVRR	Deep Ultraviolet Resonance Raman
NMR	Nuclear Magnetic Resonance
PA	Photoacid
PB	Phosphate Buffer
pHiC	pH Inducible Cation
pHiCL	pH Inducible Cationic Lipid
PLA_7	$PolyLA_7$
UV/Vis	Ultraviolet/Visible

Abstract

Alzheimer's disease, among other neurologically degenerative diseases, has been linked to protein-enzyme interactions that originate within the transmembrane domain of a cell. The lipid environment that houses these interactions lends difficulty to studying intramembrane interactions, often making for time consuming data analysis. Lengthy data interpretation on top of the rate in which protein-enzyme interactions take place creates a need for a method to overcome these obstacles. The use of lipid vesicle fusion to apply a margin of control over the time frame of interaction combined with deep probing spectroscopic techniques can minimize the interference of the lipid environment. Deep ultraviolent resonance Raman (dUVRR) is a vibrational spectroscopic technique that probes along the protein backbone that allows for removal of lipid environmental interference through background subtraction.

Lipid vesicle fusion has been demonstrated by mixing lipid vesicles comprised of oppositely charged head groups (cationic 1,2-diaurroyl-sn-glycero-3-phospho-(1-rac-glycerol) (DLPG)) and anionic 1,2-dilauroyl-sn-glycero-3-ethylphocholine (12:0 EPC) or 1,2-dimyristoyl-sn-glycero-3-ethylphocholine (14:0 EPC)) of equivalent or varying aliphatic tail length, up to a 2-carbon difference. The fluorescent dye, 8-aminonapthalene 1,3,6-trisulfonic acid (ANTS), paired with the quencher, p-xylene-bis-pyridiumbromide (DPX), are separately encased in either DLPG or 12:0 EPC/14:0 EPC, respectively, in aqueous solution, and evidence of lipid vesicle fusion is provided by monitoring fluorescence intensity of ANTS as the two solutions are mixed, resulting in the closing

proximity of ANTS and DPX observed as a decrease in fluorescence intensity. Additional evidence is provided by dynamic light scattering (DLS) measurements of both independent vesicle solutions and their mixture showing an increase in hydrodynamic radius (R_h). In addition, cohesion of similarly sized lipids is demonstrated, as DLPG (12-carbon chain) fails to fuse with cationic lipids of chain length 16 carbons or longer.

Circular dichroism (CD) is a spectroscopic technique that uses left and right-handed polarized light to obtain the overall secondary structure of proteins. Shown is the use of CD to probe the secondary structure and the changes incurred on PolyLA$_7$ (PLA$_7$), a model α-helical peptide when placed in a transmembrane or hydrophobic environment, through a change in the lipid environment. PLA$_7$ was inserted in DLPG lipid vesicles and then mixed in solution with lipid vesicles comprised of 14:0 EPC. CD spectra were obtained pre and post vesicle fusion, demonstrating the use of lipid fusion as a means to combine membrane embedded proteins of interest while still being able to observe changes that take place.

Finally, we propose an on-demand lipid fusion system in which two separate lipid vesicles could be co-suspended in solution and then chemically or photonically induced to fuse. A titration was performed to obtain the pK_a of a synthesized pH inducible cationic lipid (pHiCL). The pHiCL is a dipicolylamine with an attached 12-carbon aliphatic tail. The pHiCL was titrated while suspended in an aqueous environment and while inserted into a lipid vesicle comprised of DLPC, a net neutral lipid also with a 12-carbon length aliphatic tail. The pHiCL will be the first component of a two-part system

in which a photoacid (PA) will be used to protonate the pHiCL in solution giving rise to cationic and anionic surfaced lipid vesicles causing vesicle fusion to occur.

Introduction

In an ever aging and growing society, one increasing cause of concern is the number of individuals diagnosed with Alzheimer's disease. Alzheimer's is a neurological disease that over time affects motor functions and mental capacity. In many cases this can lead to death. A common symptom among Alzheimer's patients has been the discovery of fibril plaques that have aggregated onto the surface of the brain.[1] The fibrils these plaques are comprised of have been linked to the Amyloid Beta Precursor Protein (APP), a transmembrane protein located in the brain.[2, 3] In a healthy functioning brain, the APP is cleaved by an α-secretase in the exterior aqueous domain of the lipid bilayer. This fragment detaches from the bilayer and is metabolized by the body without any ill side effects. The formation of the fibril plaques occurs when the APP is cleaved by a β-secretase on the exterior aqueous domain of the lipid bilayer while also being cleaved by a γ-secretase in the transmembrane domain.[4] This miscleavage leads to the fragments, referred to as Amyloid Beta (Aβ), that make up the fibril plaque aggregates.[5]

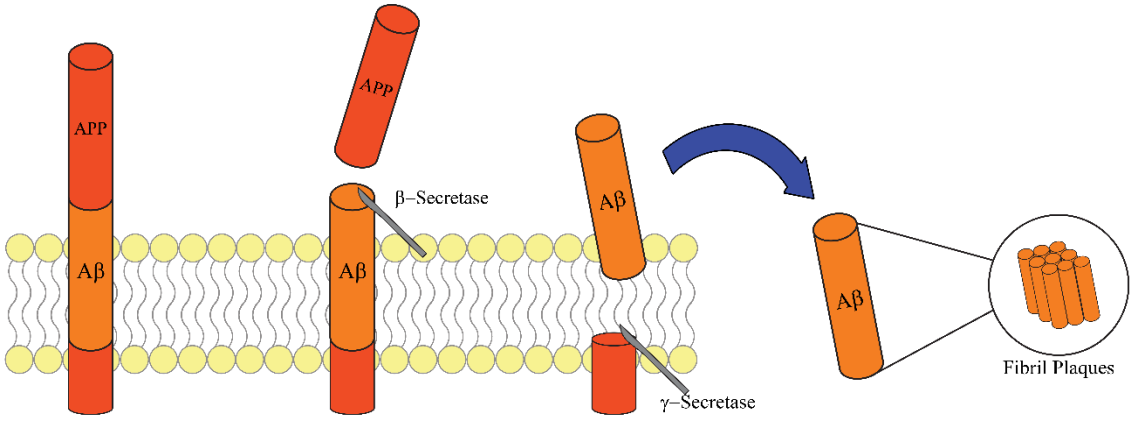

***Figure I-1**: Cleavage of Amyloid Beta Precursor Protein (APP) by a β-secretase in the aqueous domain and by a γ-secretase in the transmembrane domain leading to the formation of the Amyloid Beta (Aβ) peptide. The newly formed Aβ aggregates to form fibril plaques.*

The reason for this miscleavage and the link between the plaques it forms, and the symptoms seen in Alzheimer's patients is yet unknown but is an area of great interest to researchers.

Alzheimer's link to the membrane of a cell gives an added layer of difficulty to understanding it development. The cell membrane is a highly organized structure made of individual lipid molecules. These lipid molecules contain a hydrophilic headgroup and a hydrophobic tail. When assembled in a cellular membrane these lipid molecules form a bilayer. In the bilayer the hydrophilic headgroup will face out into the inter- or extra-cellular environment and the hydrophobic tail groups of the two layers will face each other.

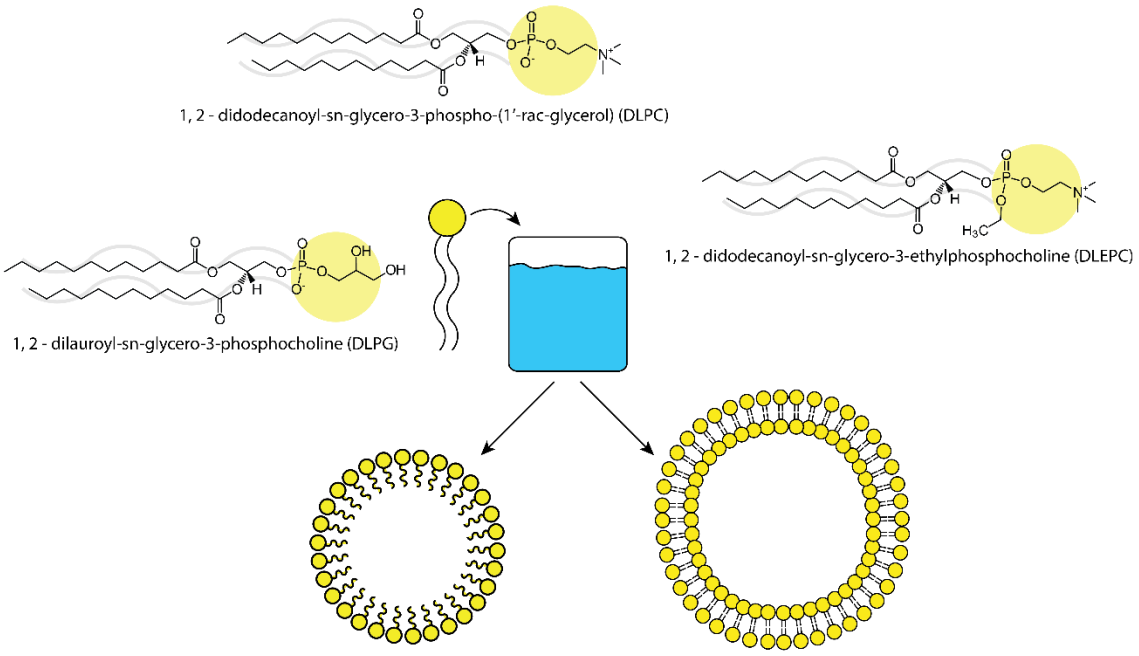

***Figure I-2**: Lipid bilayer formation and organization of hydrophilic headgroups and hydrophobic aliphatic tails in an aqueous environment.*

This arrangement allows for suspension in an aqueous environment while providing an area devoid of water for the more hydrophobic membrane proteins to reside. In the case of Alzheimer's disease, the area of interest resides in the specific region of the transmembrane portion of APP. Transmembrane proteins are proteins which span the bilayer of the cell membrane, having interactions with both the intercellular and extracellular environments. Many of these motifs act as gateways or channels and facilitate transport across the cell membrane.

As the need to understand these transmembrane proteins and their roles in degenerative diseases increases, so does the need for methods and techniques to study them. We need an understanding of the full picture of the life of a membrane protein, not just individual snapshots. This includes the mechanisms and pathways with which these

transmembrane proteins interact with their membrane hosts as well as other proteins and enzymes in the cellular environment. In comparison to transmembrane proteins' close counterpart, water soluble proteins, there is currently an expansive gap in our knowledge of transmembrane protein structure.[6] This is due to the massive amounts of data and lengthy interpretation process required by traditional protein characterization techniques when dealing with proteins inserted into a lipid bilayer. Techniques such as X-ray crystallography rely on being able to get the protein into a crystal form,[7] but with the lipid bilayer that sample will remain in a wax like state. The rate at which protein-enzyme interactions happen limits the ability of a technique like nuclear magnetic resonance (NMR) to show much more than insight into the beginning and end of the reactions as NMR requires the analyte to be at equilibrium with its environment.[8] One technique that has emerged as a front runner for the studying of transmembrane proteins in their native environment is deep-ultraviolet resonance Raman (dUVRR).

DUVRR is a vibrational technique that can probe the secondary structure of transmembrane proteins once the spectra are deconvoluted and the lipid contribution to the data is subtracted.[9] DUVRR is carried out through the use of two solid state lasers in tandem. A Ti:sapphire laser is pumped using a Nd:YLF laser giving an excitation source around 789 nm.[10] This 789 nm light and a residual collinear infrared (IR) beam are spilt and recombined using three separate harmonic generating crystals allowing for the creation of a beam with a final wavelength (λ) of 197 nm. The resulting 197 nm light is used to irradiate a sample that is being pumped between two nitinol wires forming a thin film. The nitinol wires are housed in an enclosed sample chamber being purged with a

constant flow of nitrogen. The Raman scattering emitted from the sample is refocused into a monochromator with an attached CCD camera that captures the resulting spectra.

The scattering from the interaction of the 197 nm photons with the backbone of proteins gives rise to modes that correspond to the folding and bonding structure of the protein. The major modes of interest are the amide I, II, S, and III.[11] The amide I corresponds to carbonyl stretching as well as NH bending. The amide II & III are both correlated to a combination of CN stretching and NH bending, out-of-phase and in-phase, respectively. The final mode, the amide S, has a direct correlation to the helical content of the protein structure. While dUVRR can help overcome the obstacles at the lipid environment interference, there is still the issue of the rate of interaction. This is where lipid fusion can help bridge the gap.

Lipid fusion takes place in an aqueous solution between lipid vesicles, an assembly of lipid molecules or bilayers in a spherical shape. Lipid fusion is linked to many cellular processes like intercellular transportation or viral cell infection.[12] The combining of dUVRR and liposome fusion to create an on-demand system in which a protein and its corresponding enzyme can be separate, brought together at any time, and the subsequent interactions observed in real time can open the door to better understanding of the pathways and mechanism of transmembrane proteins while in their native environment.

Chapter 1

Membrane fusion is an important biological process that aids many cellular functions such as cell division, exocytosis, and endocytosis. It can also be involved in the viral infection of a cell by transporting a membrane-enclosed virus across the cell membrane.[12] It is in this power of these lipid vesicles, or liposomes, to keep their contents contained until required that can help us better understand intermembrane proteins and their interactions with their native membrane environments.

Lipid vesicles can be formed through the sonication and gentle heating of lipids.[13] This energy input allows the lipids to align with their hydrophobic tails toward the center of the vesicle and hydrophilic head groups at the water-lipid interface. There are many classes of lipid vesicles that can be formed. For example, micelles comprise a single layer of lipids and take on a spherical shape which is devoid of water on the inside of the vesicle. It is also possible for the lipids to organize into a lipid bilayer in a spherical conformation. This class of lipid vesicle are known as liposomes. Unlike its single layered counterpart, liposomes are able to encapsulate a volume of water in the center of the vesicle. Vesicle fusion is the process by which two vesicles are brought together and made into a single vesicle structure. During the vesicle fusion process, the outer layers become one continuous structure and the inner contents of the vesicles are combined through the disruption of the lipid packing at the contact site.[14] The fusion of membranes can be initiated through the anchoring of motifs in the head groups of the outward facing lipids. These motifs are designed chemical patterns that reoccur across the

lipid surface. Their composition is based on the attraction between the functionalized head groups of the lipid and their effect has been well documented.[15, 16] The insertion of the anchored motifs into the lipid causes strain on the vesicle through disruption in the lipid packing, thus helping to induce fusion.

Fusion of lipid vesicles can be assessed using dynamic light scattering (DLS), a method used to determine the hydrodynamic radius (R_h) of a spherical particle in solution.[17] A laser is used to bombard the sample with photons. The scattering of these photons is measured as a function of the time it takes for the scattered photons to reach the detector. This time varies with the radius of the particle. As particles move in solution, they can scatter photons with different energy in relation to the incident radiation. Scattering of photons with higher energy (anti-Stokes scattering), lower energy (Stokes scattering), or the same energy (Rayleigh scattering) as the incident radiation can all occur. As the photons scatter from a smaller particle (faster motion) the photons can gain more energy than they would from a larger particle (slower motion). The diffusion coefficient (D) of the scattered photon is detected in correlation with the solvent viscosity (η), the Boltzmann constant (k), all at absolute temperature (T) allowing for the calculation of the hydrodynamic radius (R_h) by the Stokes-Einstein equation (1).

$$R_h = \frac{kT}{6\pi\eta D} \quad (1)$$

However, particle size increases can also occur from liposome aggregation as well as fusion, making it necessary to use a complimentary method for confirmation of lipid vesicle fusion.[18]

To complement the DLS data, this study uses fluorescent dyes that can be encapsulated into the vesicles. The pair of dyes used in this work to evaluate vesicle fusion are 8-aminonaphthalene-1,3,6-trisulfonic acid (ANTS) and *p*-xylene-bis-pyridiumbromide (DPX).[19] ANTS is a fluorophore that is quenched by DPX. As DPX is a dark quencher, it does not fluoresce after quenching ANTS, causing a decrease in the ANTS fluorescence intensity.

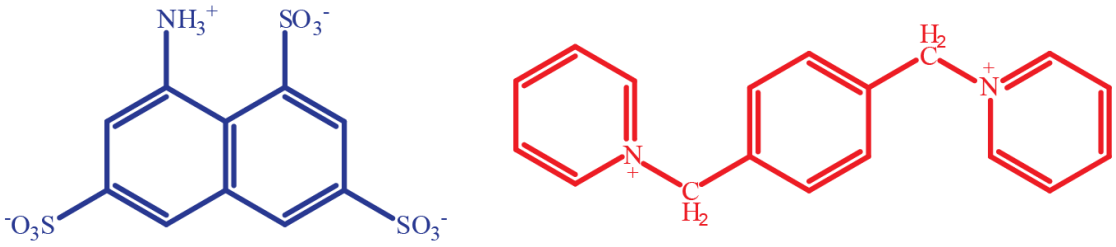

Figure 1-1*: Structure of the dyes, ANTS and DPX. The blue structure is that of 8-Aminonaphthalene-1,3,6-trisulfonic acid, disodium salt (ANTS). The red structure is that of p-xylene-bis-pyridinium bromide (DPX).*

The ANTS/DPX dyes are well suited for our goal as no chemical bonds are formed during the quenching process. Instead, the quenching is done on a collisional basis.[20] Collision quenching is quenching with its efficiency based on the distance between the fluorophore and quencher. In the case of ANTS and DPX, ~10 Å or less is needed for quenching to take place.[21] By encapsulating ANTS and DPX in separate vesicles, a decrease in fluorescence of ANTS will only happen if the two vesicles fuse, thereby allowing for DPX to come in close proximity to, and quench, ANTS. In the case of hemifusion, or combination of only the outer membrane at the vesicle-vesicle interface, the ANTS fluorescence will have no change in intensity as the dyes are not in

close enough proximity to one another. If the vesicle lipid packing were to be disrupted without fusion, the ANTS and DPX may leak out into the bulk solution and the fluorescence would once again, be unchanged due to the large dilution. An alternate method of monitoring fusion with fluorescent dyes would be to begin with both ANTS and DPX encapsulated into the same vesicle, causing the ANTS fluorescence to be initially quenched. As fusion occurs with the ANTS-DPX vesicle and a vesicle containing just phosphate buffer solution, the dilution of the ANTS-DPX into the volume of two vesicles will allow for a decrease in the proximity between ANTS and DPX, yielding an increase in the ANTS fluorescence. This allows for the dyes to freely flow between vesicles or into solution, in the case of leakage, giving a change in fluorescent intensity.

Here, the attraction of oppositely charged headgroups induces strain on the lipid packing to induce fusion without the need of additional molecules inserted in the liposomes. We also set out to ascertain the possibility of fusing lipids possessing varying hydrophobic lengths, a process also assisted by the incorporation of oppositely charged head groups. These two forms of fusion will provide us with a streamlined, highly reproducible model native environment to use as a platform to study membrane-protein interactions.

Materials and Methods

Dibasic sodium phosphate, ascorbic acid, ammonium molybdate, and perchloric acid were purchased from Fisher Scientific (Pittsburgh, PA). 1,2-diaurroyl-sn-glycero-3-phospho-(1-rac-glycerol) (DLPG), 1,2-dilauroyl-sn-glycero-3-ethylphocholine (12:0 EPC), 1,2-dimyristoyl-sn-glycero-3-ethylphocholine (14:0 EPC) and 1,2-dipalmitoyl-sn-glycero-3-ethylphocholine (16:0 EPC) were purchased from Avanti Polar Lipids (Alabaster, AL). 8-Aminonaphthalene-1,3,6-trisulfonic acid, disodium salt (ANTS), and p-xylene-bis-pyridinium bromide (DPX) were purchased from Setareh Biotech (Eugene, OR).

Fluorescent Dyes Preparation

ANTS was prepared at 25 mM in 10 mM phosphate buffer (PB; pH 7.4) and DPX was prepared at 90 mM in 10 mM PB. Dye solutions were sonicated and vortexed in 1 min increments until completely dissolved and stored at 4 °C, wrapped in aluminum foil to prevent photo bleaching.

Lipid Vesicle Preparation

DLPG was dissolved in 65:35 chloroform and methanol while 12:0, 14:0, and 16:0 EPC were dissolved in chloroform. Aliquots of the dissolved compounds of DLPG and all DLEPCs were transferred to culture tubes with the intended final dried mass being 12.5 mg per tube. The solvents were removed under a stream of argon, leaving a thin film at the bottom of the tube, and the solid was then further dried in a vacuum desiccator

overnight. Tubes of the lipids were rehydrated according to the following table (Table 1-1):

Table 1-1*: Volumes of phosphate buffer, ANTS, DPX or a combination thereof used to rehydrate previously dried down tubes of measured DLPG and EPCs of varying lengths in order to form liposomes.*

Lipid Fusion Components	Rehydration volumes of DLPG	Rehydration volumes of EPC
DLPG + 12:0 EPC	550 µL ANTS	550 µL DPX
DLPG + 12:0 EPC	275 µL ANTS + 275 µL DPX	550 µL PB
DLPG + 14:0 EPC	375 µL ANTS + 375 µL DPX	750 µL PB
DLPG + 16:0 EPC	375 µL ANTS + 375 µL DPX	750 µL PB

The tubes of rehydrating lipids were sonicated for 1 h at ~55 °C to form lipid vesicles. The newly formed lipid vesicles were extruded using an Avestin LiposoFast (Ottawa, ON) fitted with a 200 nm diameter pore filter 23 times to obtain uniform vesicle size. Lipids were centrifuged at 160,000 x g for 2 h @ 23 ℃ to remove excess dye from solution. Pellets were re-suspended with 3 mL of 10 mM PB. The Rouser phosphate assay was used to determine DLPG and DLEPCs concentration.[22]

Combination of Lipid Vesicle Solutions

Lipid vesicles of DLPG and corresponding DLEPC, in accordance with Table 1-1, were combined in a quartz cuvette with a light pathlength of 1 cm at ambient temperature in a 1:1 molar ratio with a final net volume of 3 mL. The resulting molar concentration was ~1 mM for each lipid component. Once combined in the cuvette, the two vesicle-containing solutions were mixed through gentle pipette agitation.

Fluorescence

All fluorescence measurements of ANTS/DPX fluorescence were obtained with a Varian Cary Eclipse fluorescence spectrometer (Agilent Technologies, Santa Clara, CA) with an excitation wavelength of 354 nm and an excitation/emission slit width of 5 nm. The fusion of DLPG and 12:0 EPC was monitored post mixing at time points of 5 min, 10 min, and then at 10 min increments for 1 h. As a base control, fluorescence was obtained of solutions comprising DLPG vesicles containing either ANTS or both ANTS and DPX, with both solutions being diluted with PB in volumes equivalent to the volumes of previously added 12:0 EPCs to achieve vesicle fusion at 1:1 molar ratio. The fusion of DLPG and 14:0 EPC or 16:0 EPC was monitored post mixing at time points of 0 min, 30 min, and 1 h. As a base control, fluorescence was obtained of a solution of DLPG vesicles containing ANTS and DPX diluted with PB in volumes equivalent to the volumes of previously added 14:0 or 16:0 EPCs to achieve vesicle fusion at

1:1 molar ratio. All spectra were buffer corrected and processed using MatLab (Version R2012a, MathWorks, Natick, MA).

Dynamic Light Scattering

Dynamic light scattering (DLS) was performed on a DynaPro (Wyatt Technology Corp. Santa Barbara, CA). Hydrodynamic radius measurements were taken for DLPG and corresponding DLEPCs. DLS was performed after extrusion, pellet resuspension, and after the combining of DLPG and 12:0 EPC lipid vesicles (1 h post fusion and overnight at ambient temperature). All 14:0 EPC and 16:0 EPC samples were run prior to solution mixing and 1 h after mixing. 5 µL aliquots of all samples were diluted with 225 µL of 18.2 MΩ water previously filtered through a 0.1 µm Whatman filter, then vortexed for 10 seconds. All samples were scanned 23 times at 1 scan per 5 seconds, then averaged by DynaPro system automated software.

Results

When DLPG vesicles containing ANTS and 12:0 EPC vesicles containing DPX are mixed in solution, a decrease in fluorescence intensity is seen within 5 min of combination, and the fluorescence intensity continues to slowly decrease over 60 min as shown in Figure 1-2.

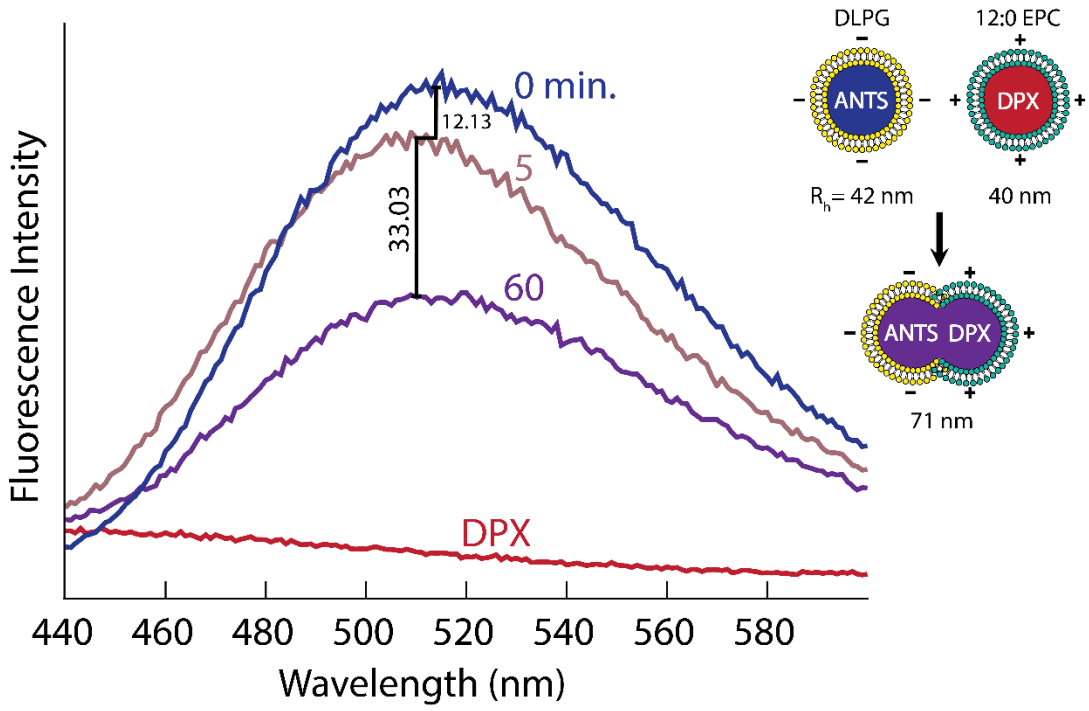

***Figure 1-2**: **(Left)** Fluorescence spectra showing the quenching of ANTS by DPX. The red line represents DPX in 12:0 EPC whereas the blue line represents ANTS in DLPG. The pink and purple lines represent the mixture at 5 and 60 min, respectively, indicating a loss of fluorescence from collisional quenching after fusion has occurred from mixing in solution at a 1:1 molar ratio. All spectra were obtained using an excitation of 354 nm with an excitation/emission slit width of 5 nm. **(Right)** Representation of DLS data pre- and post-fusion. The yellow vesicle (top-left) represents DLPG vesicles containing ANTS fusion. The teal vesicle (top-right) represents 12:0 EPC vesicle containing DPX prior to fusion. The yellow/teal vesicle (bottom-right) represents a newly formed vesicle compromised of both DLPG and 12:0 EPC lipids after fusion has taken place.*

The combination of the DLPG vesicles containing ANTS-DPX and 12:0 EPC vesicles containing phosphate buffer results in an increase in intensity of the ANTS fluorescence within 5 min of mixing the vesicles solutions and maintains the same fluorescence intensity over the course of 60 min as shown in Figure 1-3. In combination with the fluorescent dye pairing, DLS was also used. The DLS data represented on the right side of Figures 1-2 and Figure 1-3, shows an approximate doubling in the vesicle

size for both fusion trials containing lipids of equivalent length. The initial R_h of 40-42 nm for both DLPG and 12:0 EPC respectively, combine in a new formed vesicle giving rise to a new R_h of 71 nm (Figure 1-2). Following the same pattern, the initial R_h of 31 nm for both DLPG and 12:0 EPC combine in a new formed vesicle giving rise to a new R_h of 57 (Figure 1-3).

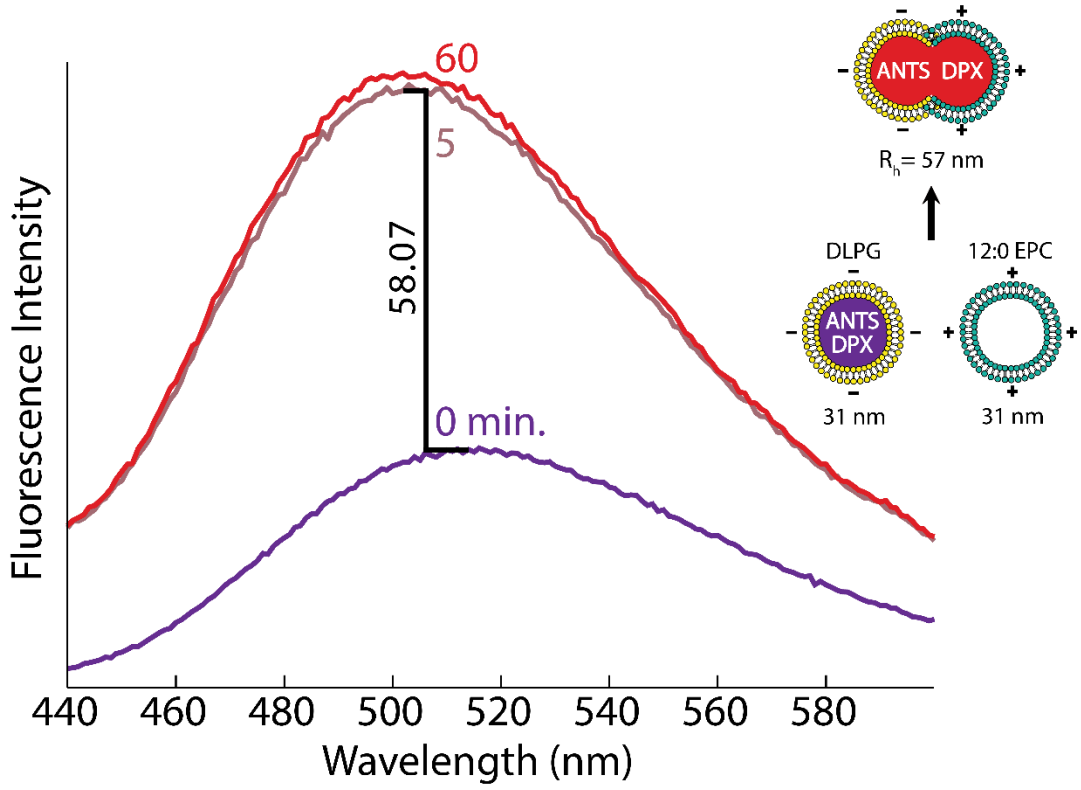

***Figure 1-3**: Fluorescence spectra showing the quenching of ANTS by DPX prior to fusion. The purple line indicates ANTS initial quenching by DPX from co-encapsulation in DLPG vesicles prefusion. The pink and red lines show an increase in ANTS fluorescence at 5 and 60 min due to dilution by way of vesicle fusion between DLPG and 12:0 EPC lipid vesicles containing phosphate buffer after being mixed in solution at a 1:1 molar ratio. All spectra were obtained using an excitation of 354 nm with an excitation/emission slit width of 5 nm. **(Right)** Representation of DLS data pre- and post-fusion. The yellow vesicle (bottom-left) represents DLPG vesicles containing both ANTS and DPX prior to fusion. The teal vesicle (bottom-right) represents 12:0 EPC vesicle containing phosphate buffer prior to fusion. The yellow/teal vesicle (top-right) represents*

a newly formed vesicle compromised of both DLPG and 12:0 EPC lipids after fusion has taken place.

The method of fusion discussed above was also applied to a system in which the same anionic lipid, DLPG, was used in an attempt to fuse with cationic lipids containing 2 and 4 carbons more in length, 14:0 EPC and 16:0 EPC. When DLPG liposomes containing ANTS/DPX were mixed in solution with 14:0 EPC liposomes containing phosphate buffer, we see an immediate increase in ANTS fluorescent intensity that stays at the increased intensity over the course of 60 min of monitoring as shown in Figure 1-4. The DLS data represented on the right side of Figure 1-4 shows that, unlike the fusion of vesicles of equivalent length, there is increase in size from the 14:0 EPC vesicles from a R_h of 35 nm to 41 nm. This is the opposite change for the DLPG vesicles that were initially measured with a R_h of 69 nm. Previously the change in R_h was seen as a sum of both vesicle components. Here it is shown to be the average between both initial components R_h.

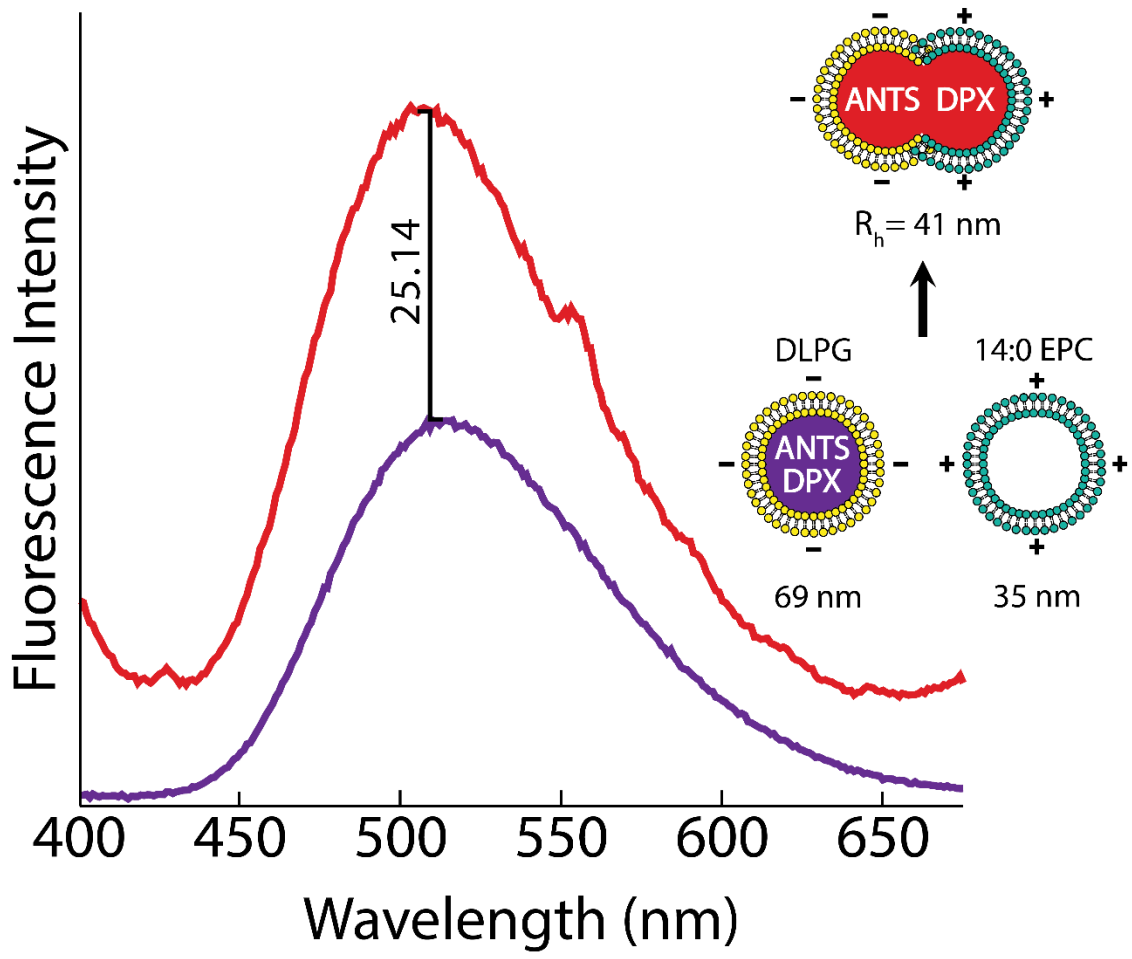

***Figure 1-4**: **(Left)** Fluorescence spectra showing the quenching of ANTS by DPX prior to fusion. The purple line indicates ANTS initial quenching by DPX from co-encapsulation in DLPG lipid vesicles prefusion. The red line shows an increase in ANTS fluorescence due to dilution by way of vesicle fusion between DLPG and 14:0 EPC lipid vesicles being mixed in solution at a 1:1 molar ratio. All spectra were obtained using an excitation of 354 nm with an excitation/emission slit width of 5 nm. **(Right)** Representation of DLS data pre- and post-fusion. The yellow vesicle (bottom) represents DLPG vesicles containing both ANTS and DPX prior to fusion. The teal vesicle (bottom-right) represents 14:0 EPC vesicle containing phosphate buffer prior to fusion. The yellow/teal vesicle (top-right) represents a newly formed vesicle compromised of both DLPG and 14:0 EPC lipids after fusion has taken place.*

The same cannot be said for when DLPG liposomes containing ANTS/DPX were mixed in solution with 16:0 EPC vesicles containing phosphate buffer (Figure 1-5). The fluorescent intensity did not change besides an increased baseline across the entire spectrum and a shoulder peak that appears at 560 nm in both fusion spectra between DLPG and 14:0 EPC or 16:0 EPC, respectively. This increased baseline is seen in all spectra involving lipid vesicle fusion discussed. The DLS data shown in Figure 1-5 mimics the fluorescence data in the lack of change in vesicles sizes between pre- and post-fusion attempt. The DLPG (R_h of 57 nm) combines with the 16:0 EPC (R_h of 69 nm) combines to an average R_h of 59 nm after fusion is induced.

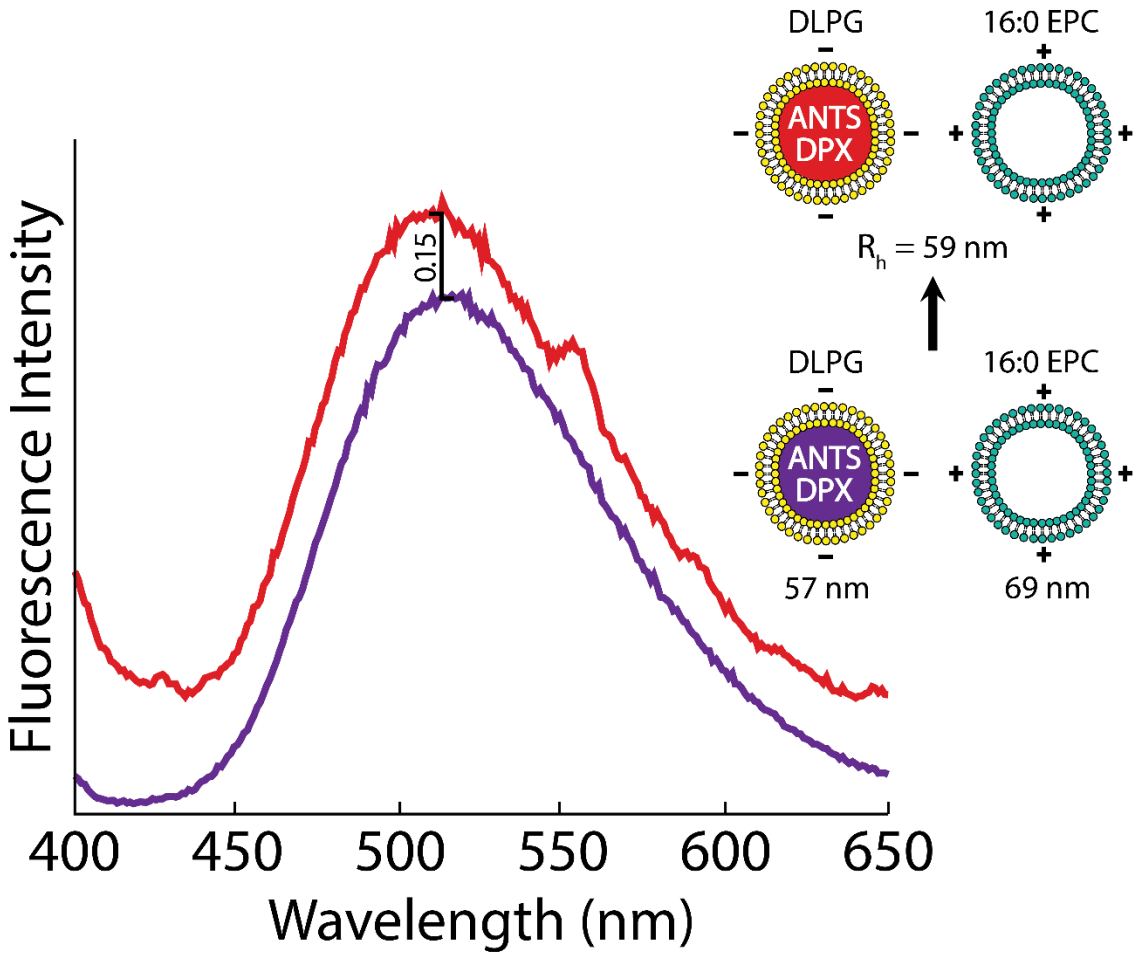

***Figure 1-5**: **(Left)** Fluorescence spectra showing the quenching of ANTS by DPX prior to attempting fusion. The purple line indicates ANTS initial quenching by DPX from co-encapsulation in DLPG vesicles prefusion. The red line shows a slight increase in fluorescence caused by increased scattering of photons, not likely lipid vesicle fusion as previously shown. All spectra were obtained using an excitation of 354 nm with an excitation/emission slit width of 5 nm. **(Right)** Representation of DLS data pre- and post-mixing of solutions containing DLPG and 16:0 EPC lipid vesicles in a 1:1 molar ratio. The yellow vesicle (bottom) represents DLPG vesicles containing both ANTS and DPX prior to solution mixing. The teal vesicle (bottom-right) represents 16:0 EPC vesicle containing phosphate buffer prior to fusion. The yellow and teal vesicle (top-right) represents a lack of fusion taking place between DLPG and 16:0 EPC.*

Discussion

The decrease in ANTS fluorescent intensity, as observed during the mixing of DLPG vesicles containing ANTS with DLEPC vesicles containing DPX, is a much slower and gradual decline as compared to the abrupt and relativity stable increase we see in the fusion control study of DLPG vesicles containing ANTS/DPX with phosphate buffer encapsulated DLEPC vesicles. We propose that this slow loss of intensity is a result of the ANTS and DPX mixing over the course of the 60 min observation window, as compared to simple dilution of the constituents in the control study. Leakage of encapsulated content is not uncommon when vesicle fusion occurs. This is usually due to the method in which fusion is induced. The disruption of the lipid bilayer causes an opening of the vesicle before reassembly can occur with the opposing vesicle. Here, we do not detect vesicle leakage, which would be evidenced by an increase in the fluorescence intensity of ANTS as it dissociates further away from the DPX. The method described above is believed to go through a hemifusion stage, as opposed to the more direct opening of the vesicles and reassembly. The hemifusion of the two vesicles is a melding at the point of surface interface interaction where a mixing of the two vesicles takes place, eventually leading to separation of the two newly mixed bilayers, allowing for the previously encapsulated contents to flow together without leakage. The DLS data for both fusion experiments involving DLPG and DLEPC alludes to an increase in individual lipid vesicle size that is equivalent to the sum of the two separate vesicles combined after mixing of the vesicles takes place.

The lack of significant change in lipid vesicle radius for the attempted fusion of DPLG with 16:0 EPC confirms what the fluorescence data shows; failure to induce fusion. In the previous fusion of lipid vesicles, successful inducing of fusion involved an abrupt increase in fluorescence intensity coupled with a summation of the vesicle hydrodynamic radius of the two separate vesicles being fused. While there is a slight change in measured DLS data, this could be simply from averaging of the two separate types of vesicles radii as they are combined in solution. This observation viewed alongside the absence of increase in ANTS fluorescence by dilution into a larger inter volume that results from two fused lipid vesicles concludes a lack of fusion taking place. The inability of DLPG to fuse successfully with 16:0 EPC could be caused by lack of energy or applied strain that is placed on the packing system of the lipid bilayers. It is possible that the extended aliphatic tail of 16:0 EPC is lending overall stability to the lipid bilayer allowing it to withstand the external forces applied with its attraction to DLPG.

The DLPG mixed with 14:0 EPC paints a very different picture than the attempt with 16:0 EPC. There is a sharp and immediate increase in the fluorescent intensity of ANTS, which is consistent with successful vesicle fusion, but the most interesting occurrence happens when we look at the DLS. Previously, it was shown that when fusion is achieved between two lipid vesicles of equivalent length, the hydrodynamic radius of the newly formed vesicle is shown to be the total sum of the two separate vesicles, but in this case, we determine the new vesicle size to be a median of the two separate vesicles fused. The two-carbon-length difference between DLPG and 14:0 EPC may be allowing

for a canopy effect to take place. This canopy would be comprised of the DLPG slotting in between the 14:0 EPC and sinking below the headgroup of 14:0 EPC, allowing for the bottom of the lipid tails to be level with each other while the headgroups maintain a continuous interface with the aqueous environment. If the 14:0 EPC were to completely close over the DLPG, I believe we would not have seen a change in the DLS from the initial size of 14:0 EPC having a R_h of 35 nm. This spacing between the 14:0 EPC by the DLPG may give the surface of the lipid vesicle a pitted look, similar to that of a golf ball. This canopy effect seems to also allow for tighter packing of the lipids together which would be seen by the averaging between the two separate vesicles as opposed to the sum of the vesicles after fusion.

In conclusion, a method of lipid vesicle fusion has been shown that can bypass typical complex protein initiated, or motif embedded induced lipid bilayer destabilization to allow for fusion to take place. This new method uses oppositely charged headgroups to bring together and open the lipid vesicles to form a new lipid vesicle allowing for a mixing of the encapsulated contents. Fusion has been shown to be possible between to vesicles with equivalent lipid length as well as lipids that differ by up to two carbons. Lipids differing by more than two carbons in length appear to be too stable for this method to induce fusion, needing a larger external force to disrupt the lipid bilayer packing in order for fusion to take place.

Chapter 2

There are two major obstacles faced while investigating transmembrane proteins in their native environment: the speed at which interactions within the membrane take place and the extraction of viable data from the interference of the membrane itself.[23, 24] A possible pathway to circumvent these roadblocks is the use of lipid membrane fusion, a process discussed in the previous chapter, combined with circular dichroism (CD).

Circular dichroism is a spectroscopic method that uses left and right-handed circularly polarized UV light to probe the bulk secondary structure composition of proteins. The CD spectra of a protein is the sum of the responses from the different secondary structures contained within that protein. The three common types of protein secondary structure give rise to unique CD responses.[25, 26] An α-helical structured protein will show a negative feature at 208 and 222 nm along with a positive feature at 193 nm. β-sheets exhibit a positive feature at 195 nm and a negative feature at 218 nm, while disordered folding shows little to no features, with a negative dip at 195 nm after which the spectrum levels off. While CD gives insight into the secondary structure of proteins and can be deconvoluted into its constituent parts, much like dUVRR, the distinction between the two techniques is in the details. The modes that arise in dUVRR spectra provide more localized, focused changes to specific traits of the protein secondary structure, yet the technique requires an increased data collection time. CD may not provide the same level of secondary structure detail as dUVRR, but sample preparation and data collection are quick and cost efficient. These advantages make CD a good tool

for initial fusion experiments as only a global look at secondary structure changes between unfused and fused vesicle states is needed.

To demonstrate that membrane imbedded proteins will laterally diffuse through the membranes of a fused vesicle system a model peptide, PolyLA$_7$, was used (Figure 2-1). PolyLA$_7$ (PLA$_7$) is a synthesized peptide comprised of 7 alternating units each of leucine and alanine with a tryptophan at the C-terminus.

Poly(LA)$_7$	**KKLALALALALALAKKW**

***Figure 2-1**: Amino acid sequence of Poly(LA)$_7$ peptide*

This sequence allows PLA$_7$ to spontaneously insert into an anionic lipid bilayer at low concentrations. The move from a hydrophilic environment to a hydrophobic environment causes the PLA$_7$ to transition from a disordered state to an alpha helical configuration. The C-terminal tryptophan serves two purposes: to help anchor PLA$_7$ in the lipid membrane and act as an environmental marker for membrane insertion.

Here, studies monitoring the structural changes of PLA$_7$ when inserted into DLPG and fused with lipid vesicles of varying length are presented.

Materials and Methods

Dibasic sodium phosphate, ascorbic acid, ammonium molybdate, and perchloric acid were purchased from Fisher Scientific (Pittsburgh, PA). 1,2-diaurroyl-sn-glycero-3-phospho-(1-rac-glycerol) (DLPG), 1,2-dilauroyl-sn-glycero-3-ethylphocholine (12:0 EPC), 1,2-dimyristoyl-sn-glycero-3-ethylphocholine (14:0 EPC)) were purchased from

Avanti Polar Lipids (Alabaster, AL). PLA_7 was purchased from Atlantic Peptides (Lewisburg, PA).

Lipid Vesicle Preparation

All lipid vesicles of DLPG, 12:0 EPC, and 14:0 EPC were prepared in the same manner as previously described in Chapter 2 materials and methods section with the following changes: All lipids were rehydrated with only phosphate buffer and after extrusion the DLPG vesicle solution was diluted to 40 mL with phosphate buffer.

$PolyLA_7$ prep and Insertion

Four tubes containing 0.05 mg of PLA_7 previously dried under a stream of Ar were each rehydrated through combination with 5 mL of the above mentioned prepared DLPG lipid vesicle solution. The resulting molar concentration of peptide:lipid was 1:100. The remaining 20 mL of DLPG solution was used as blanks for data collection purposes. The tubes were left covered overnight at ambient temperature on the bench top to fully equilibrate. Then all tubes were combined and spun at 160,000 x g for 2 h @ 4 °C. The formed pellet was resuspended in 5 mL of phosphate buffer. The Rouser phosphate assay was used to determine lipid concentration of DLPG, 12:0 EPC, and 14:0 EPC[22]. Fluorescence of tryptophan at a concentration of 0.1 mg/mL in an aqueous solution was obtained with an excitation at 295 nm. Fluorescence was also used to confirm insertion of PLA_7 into the DLPG lipid vesicle. All fluorescence measurements were taken on a Varian Cary Eclipse fluorescence spectrometer (Agilent Technologies, Santa Clara, CA).

Circular Dichroism

Spectra of the DLPG inserted PLA_7 were obtained pre- and post-fusion with 12:0 EPC and 14:0 EPC. In addition, a sample of each lipid vesicle solution collected to provide a blank used for spectra correction. All spectra were collected using a Jasco J-710 Spectrophotometer. Samples were placed in a 1 mm pathlength quartz cuvette (Hellma Analytics, Plainview, NY) and scanned from 250 nm to 190 nm. Scanning speed was set to 50 nm/min with a total accumulation of 5 scans. Each sample's 5 scans were averaged and then all PLA_7 spectra were background corrected through subtraction of a DLPG blank spectrum. All spectra processed and corrected using MatLab (Version R2012a, MathWorks, Natick, MA).

Results

PLA_7 is a model α-helical peptide when embedded into a hydrophobic environment. After being left overnight to encourage spontaneous insertion of PLA_7 into an anionic lipid, DLPG, fluorescence of the sample with respect to the attached tryptophan was collected (Figure 2-2). There is a blue shift seen in the tryptophan fluorescence as it transitions from an aqueous to hydrophobic environment. Fluorescence was also collected after vesicle fusion had taken place. No shift in emission wavelength is seen, but there is a decrease in fluorescence intensity.

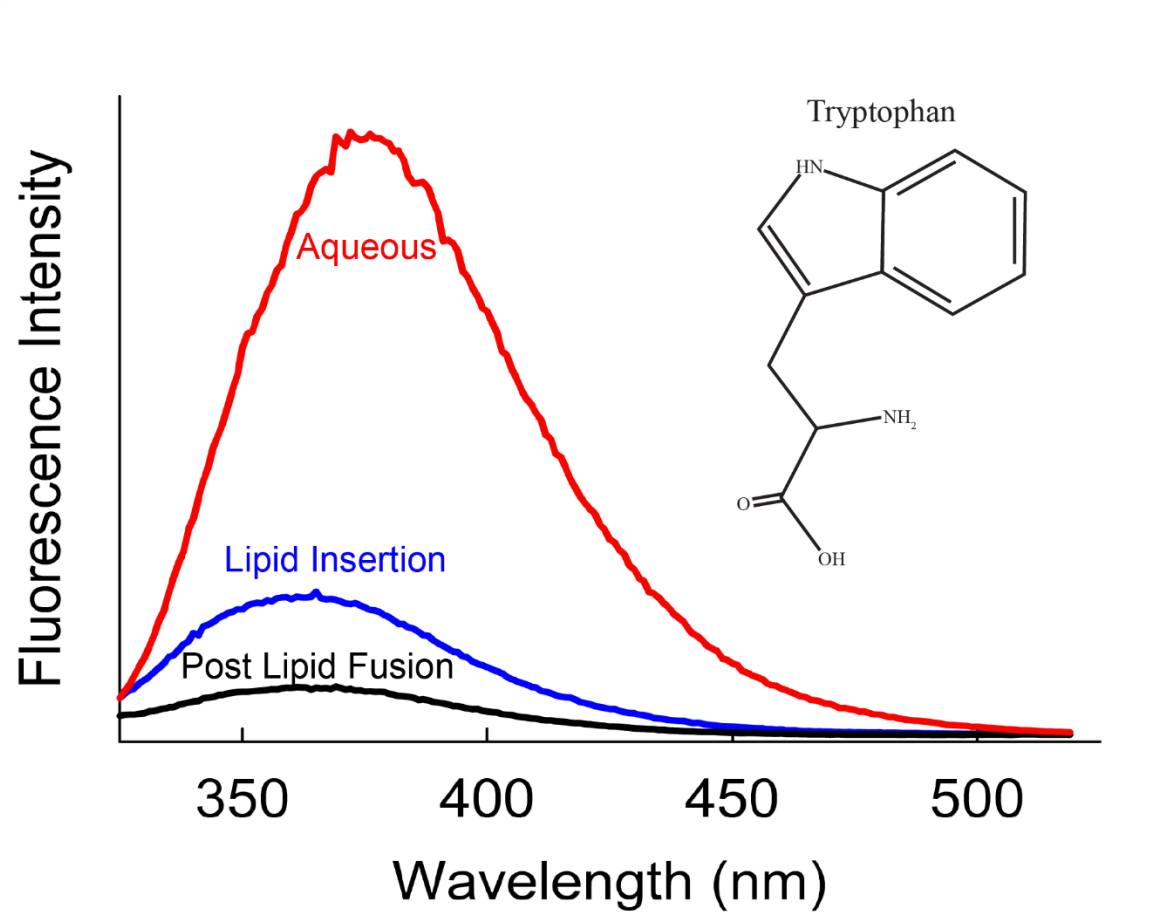

***Figure 2-2**: Fluorescence spectra of tryptophan at the C-terminal of PLA_7 used as an environmental marker. The red line shows the tryptophan at 0.1 mg/mL in an aqueous environment. The blue shows a shift to a shorter wavelength as the tryptophan on the C-terminus of the PLA_7 enters into a hydrophobic environment, in this case, insertion into DLPG comprised lipid vesicles. The black line confirms that even after vesicle fusion has taken place, the PLA_7 remains anchored in the DLPG vesicles therefore maintaining a hydrophobic environment surrounding tryptophan. All spectra were obtained using an excitation of 295 nm.*

CD was used to determine the PLA_7 secondary structure. The resulting spectra was corrected through subtraction of the lipid bilayer contribution. The CD spectra of PLA_7 shows three distinct features: a positive peak maximum at 193 nm and two negative features at 208 nm and 225 nm (Figure 2-3). The solution containing the DLPG with inserted PLA_7 was combined with a solution containing

14:0 EPC lipid vesicles containing only phosphate buffer to induce fusion, as schematically shown in Figure 2-3. The fusion of the varying-length lipids created a new mixed environment for the PLA_7 to equilibrate within, after which the changes were observed through CD.

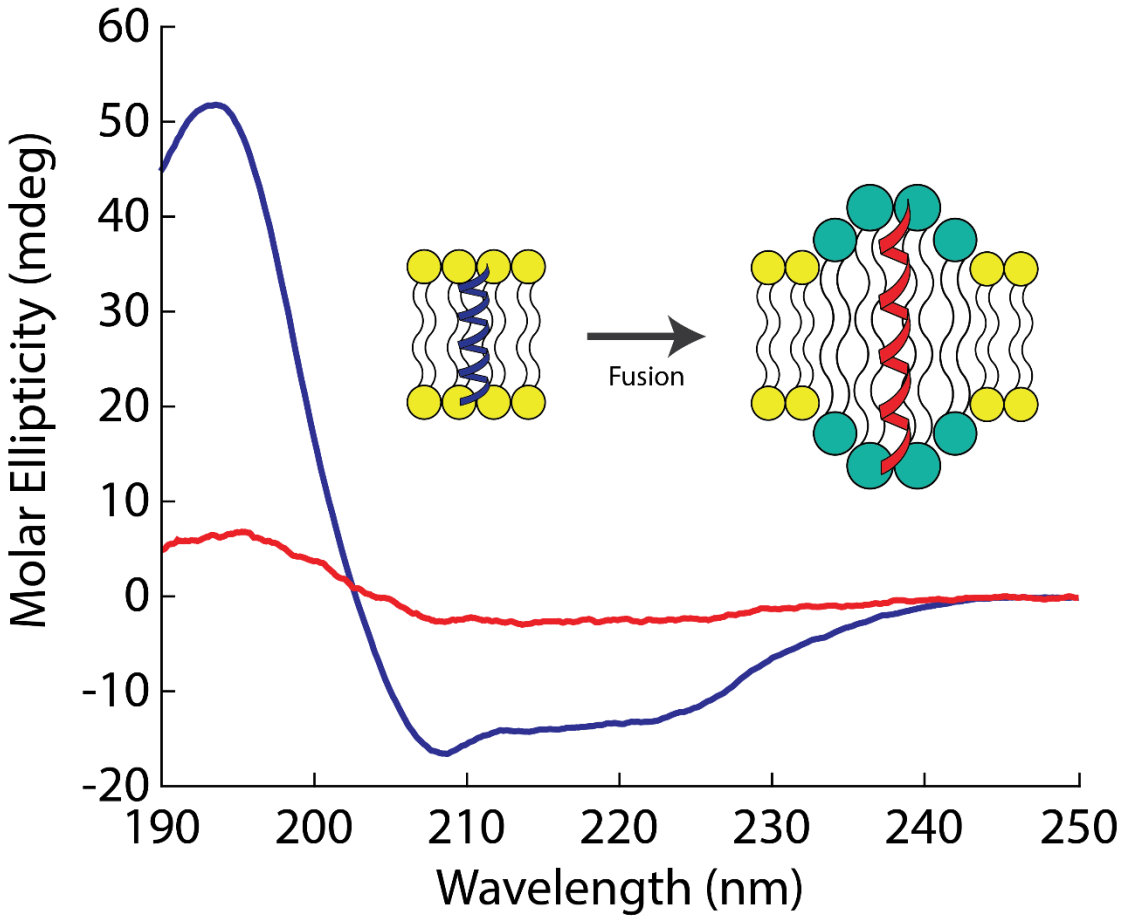

***Figure 2-3**: Circular dichroism spectra of PLA_7. The blue line shows PLA_7 inserted into lipid vesicles comprised of DLPG prior to lipid vesicle fusion taking place. The red line shows PLA_7 post lipid vesicle fusion taking place between the DLPG and 14:0 EPC lipid vesicles.*

Notably, there is a decrease in the pre-fusion features. While a maximum peak is still clearly visible around 194 nm, the two negative features have leveled

off, approaching 0 ellipticity. Even with the dramatic loss of negative features, there is still an observable negative ellipticity around 208 nm and 226 nm.

DLS was also used in concert with CD to validate that fusion had taken place between the DLPG and 14:0 EPC vesicles. DLPG showed a R_h of 36 nm which rose to 81 nm after the insertion of PLA_7. The 14:0 EPC vesicles were determined to have a R_h of 53 nm. The R_h of the newly formed vesicles swelled to have a R_h of 121 nm post-fusion.

Discussion

Circular dichroism has been widely used to determine the secondary structure of proteins in aqueous solution as well as lipid membrane environments.[26] The ability to remove the interference of the lipid membrane in studies involving transmembrane substrates is one of its greatest strengths, along with being (in general) cheaper, faster, and less data-intensive than NMR or X-ray crystallography. These advantages come at the cost of specific protein structural details, but still makes CD a great starting point for our purpose of validating a new method of lipid vesicle fusion.

Circular dichroism was used to observe PLA_7 in a hydrophilic environment, specifically, DLPG lipid vesicles. The CD spectra exhibits a positive mode at 193 nm and two negative modes at 208 and 225 nm, which correlates with a primary α-helical secondary structure. After lipid fusion was induced with 14:0 EPC lipid vesicles, there is a reduction of the two previous negative features as they approach 0 ellipticity. The modes become faint but can still be observed. The positive mode at 193nm is also vastly reduced. Despite the less intense features, this spectrum is still indicative of an α-helical

secondary structure, but one that is elongated or stretched.[27] As the two lipid vesicles fuse it can be imagined that there is a mixing of the different length lipids throughout the newly formed vesicle. Indeed, we propose that the PLA_7 is stretched in the presence of this new, longer lipid chain to maintain an anchor point at the lipid-aqueous interface. This stretching results in a weakening of the H- bonds along the backbone of PLA_7, in turn causing a decrease in the CD response while maintaining its α-helical secondary structure.

The fusion of the vesicles was confirmed through the change in PLA_7 as well as the DLS data. The DLPG with inserted PLA_7 with a R_h of 81 nm and 14:0 EPC at 53 nm increased to an average R_h of 121 nm after vesicle mixing and fusion. Interestingly, we see a size change in the vesicles that is equal to the sum of the vesicle groups being fused. The change in size of the vesicles pre- and post-fusion is consistent with fusion induced between lipid vesicles as discussed in the previous chapter.

In conclusion, lipid vesicle fusion in conjunction with CD was found to be able to show a change in a model α-helical peptide, PLA_7, as its secondary structure changed. This also shows that it can be possible to bring contents that are embedded in the transmembrane domain of separate lipid bilayer together as the bilayers mix though fusion.

Chapter 3

Using the knowledge of oppositely charged vesicles as a means to induce fusion and the ability to view changes in the secondary structure of an embedded transmembrane protein through spectroscopic means opens the door to true photoinduced on-demand vesicle fusion. On-demand fusion will allow for increased control over the intermembrane interactions by inducing fusion in a desired time frame for observation.

The substrates of interest would be inserted into neutrally charged vesicles with a set of complementary molecules embedded as a repeating motif across the vesicles surface. One set of lipid vesicles would contain a photoacid (PA), a molecule that can be photo transitioned to an excited state causing deprotonation. The proton lost by the PA can be captured by a pH inducible cation (pHiC) embedded in another set of lipid vesicles. The pHiC, when protonated, will transition to a net positive charge while the PA will now be negatively charged. Unlike the lipid fusion methods previously described, these two sets of vesicles can be placed in solution together without fusion being initiated until the specific target time frame is met.

This photoinitiated on-demand fusion in conjunction with dUVRR is where the potential of this method for intermembrane studies can prove to be most beneficial. When dUVRR data is collected, the sample solution is pumped from a sample reservoir through a system of tubing that results in the sample cascading in a thin sheet between 2 parallel needles and then recollected to continue circulation. This method of circulation helps prevent degradation of samples from continually being hit by the light source. In the case

of on-demand fusion, the solution containing the 2 groups of lipids vesicles to be fused could be circulated through the system and the external light source used to photo initiate the fusion focused to a small area of the sample reservoir. As the sample cycles and fusion takes place, the dUVRR spectra will slowly change and evolve as a result the intermembrane interactions start to take place.

Preliminary data finding a suitable pHiC is presented with the goal of finding the pK_a in aqueous solution as well as when embedded in a lipid membrane. The pH inducible cationic lipid (pHiCL) in question is a dipicolylamine with an attached 12 carbon aliphatic tail to mimic the lipid tail of DLPG in length and in traits for it to

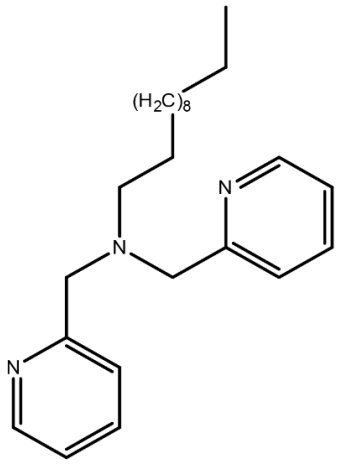

Figure 3-1*: Structure of pH inducible cationic lipid (pHiCL)*

be inserted into a lipid membrane while leaving the 2 amines exposed to the aqueous environment for protonation by the PA as shown in Figure 3-1.

Materials and Methods

Dibasic sodium phosphate, sodium hydroxide, hydrochloric acid, acetonitrile, citric acid were purchased from Fisher Scientific (Pittsburgh, PA). 1,2-diauroyl-sn-glycero-3-phosphocholine (DLPC) was purchased from Avanti Polar Lipids (Alabaster, AL). pH-inducible cation lipid (pHiCL) was synthesized by Dr. Timothy Glass' research group (University of Missouri-Columbia).

pHiCL Sample Preparation and Titration

pHiCL in Non-Lipid Environment

Into a glass culture tube, 1.75 mg (2 µL) of the neat pHiCL was weighed and then suspended in 3 mL of 50:50 ACN:PB. The tube was gently vortexed, and the solution was transferred to a quartz cuvette. The solution pH was adjusted to 10 to start the titration, moving toward a pH of 4 in increments of 0.2 - 0.3 pH using HCL. Once at a pH of 4, using NaOH, the solution was returned to a pH of 10 in increments of 0.2 – 0.3 pH. Absorbance of the pHiCL sample solution was acquired using a Varian Cary 50 Bio UV/Vis spectrometer (Agilent, Santa Clara, CA) at each change in pH from alkaline to acidic conditions and back. Absorbance at 270 nm was plotted and fitted using MatLab (Version R2012a, MathWorks, Natick, MA). The first derivative of the fitted curve was used to determine pK_a at the inflection point.

pHiCL in Lipid Environment

Into a tube containing 3.125 mg of DLPC, previously measured and dried under a stream of Ar as previously discussed in Chapter 1, was added 1.75 mg (2 µL) of the neat pHiCL. The DPLC/pHiCL was rehydrated using 550 µL of citrate-phosphate buffer (CPB) and gently sonicated for 1 h at ~55 °C to form lipid vesicles. The newly formed lipid vesicles were extruded using an Avestin LiposoFast (Ottawa, ON) fitted with a 200 nm diameter pore filter 23 times to obtain uniform vesicle size. The solution pH was adjusted to 10 to start the titration, moving toward a pH of 4 in increments of 0.2 - 0.3 pH using HCl. Once at a pH of 4, using NaOH, the solution was returned to a pH of 10 in increments of 0.2 – 0.3 pH. Absorbance of the pHiCL in DPLC vesicle sample solution was acquired by a Varian Cary 50 Bio UV/Vis spectrometer (Agilent Technologies, Santa Clara, CA) at each change in pH from alkaline to acidic conditions and back. Absorbance at 270 nm was plotted and fitted using MatLab (Version R2012a, MathWorks Natick, MA).

Results

The first step taken on the path to finding a compatible PA to go along with the synthesized pHiCL was to determine the pK_a. A titration was carried out with the pHiCL in an aqueous environment and inserted into a lipid environment to account for any changes the proximity to the lipid surface may have on the accessibility of the dipicolylamine (Figure 3-2).

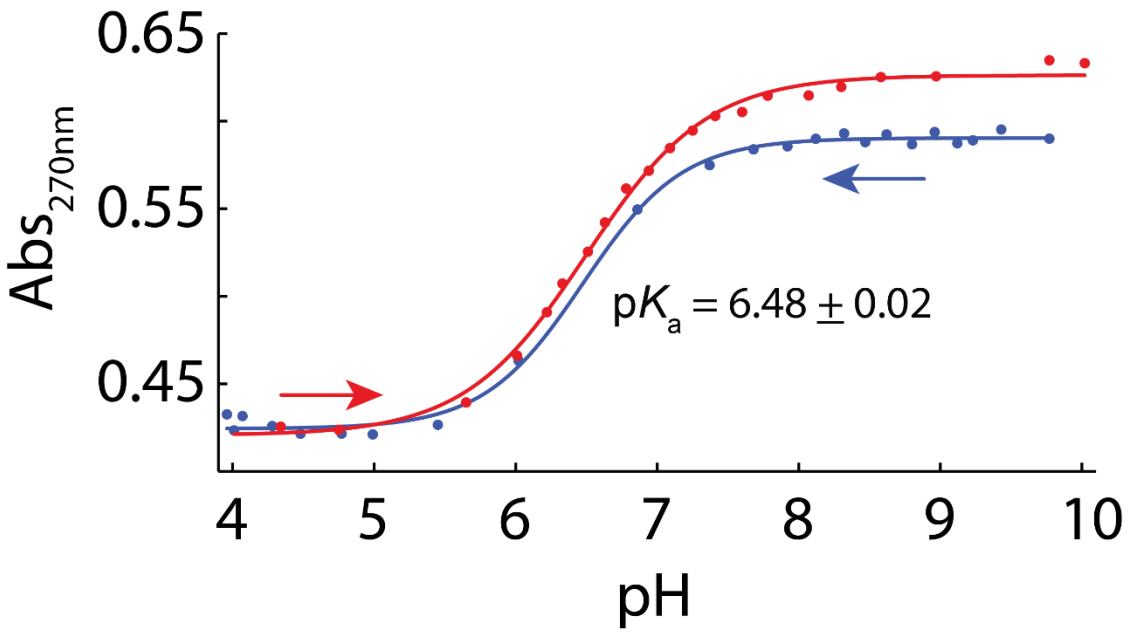

***Figure 3-2**: Titration of pHiCL in 50:50 ACN:PB. The blue fitted line represents the titration starting at alkaline (pH 10) and moving to acidic (pH 4) conditions. The red fitted line represents the reverse titration of pHiCL, moving from acidic conditions and returning to alkaline conditions.*

The titration in the absence of lipids starts at a pH 10 moving towards pH 4 by the addition of small aliquots of a HCl solution and then reverting towards alkaline conditions with the addition of NaOH aliquots. The forward and reverse titrations show uniform titration curves. The titration curves were fitted using a sigmoidal plot to calculate inflection points from the first derivate of both curves, respectively. Thus, the average pK_a value of 6.48 $\pm$ 0.02 was determined.

Next a titration of the pHiCL inserted into lipid vesicles comprising 1,2-dilauroyl-sn-glycero-3-phosphocholine (DLPC). DLPC was chosen due to its 12 carbon aliphatic tails and its net neutral charge as to minimize interference with the oppositely charged headgroup affinity needed for fusion to take place. The titration of pHiCL inserted into

DLPC gives no noticeable indication of a reversible protonation/deprotonation of the dipicolylamine taking place. As shown in Figure 3-3, the titration starts at pH 10 moving to pH 4 with the addition of small aliquots of HCl, and a drop in absorbance is observed between pH 4 and 5. The reverse titration continues the trend of a declining absorbance as it returns to a more alkaline environment of pH 10 by the addition of small aliquots of NaOH.

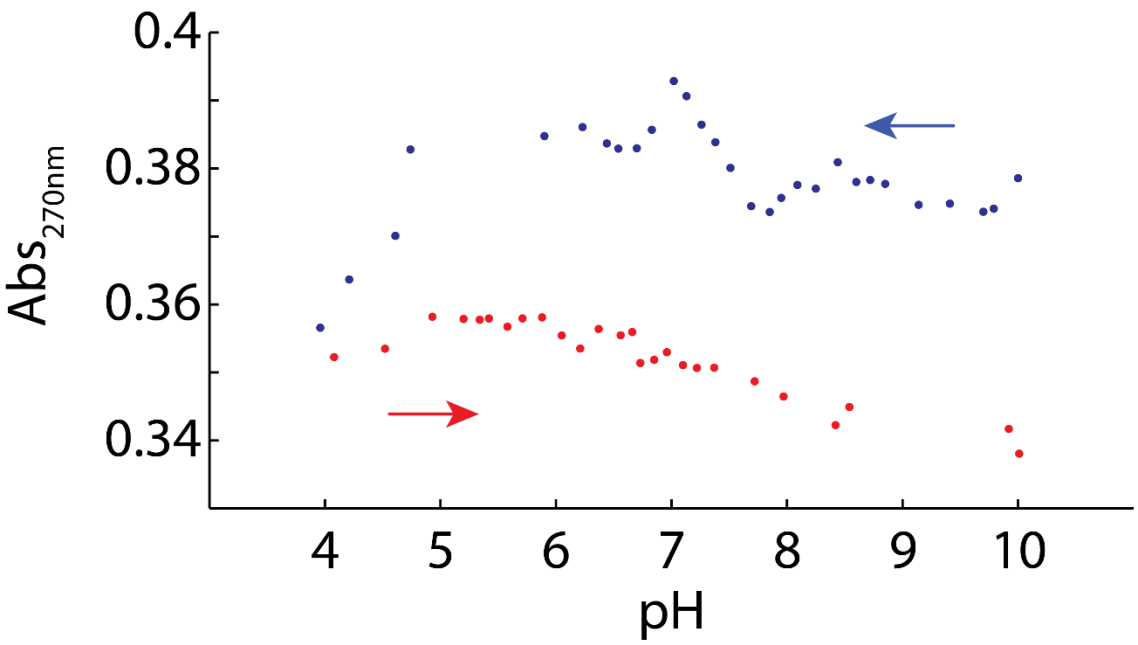

Figure 3-3*: Titration of pHiCL inserted in DLPC lipid vesicles carried out in CPB. The blue data points represent the titration starting at alkaline (pH 10) and moving to acidic (pH 4) conditions. The red data points represent the reverse titration, moving from acidic conditions and returning to alkaline conditions.*

Discussion

The ability to understand and observe transmembrane protein interactions in their native lipid environment in real time can greatly help in the fight against poorly understood mechanisms of diseases that result from these intermembrane interactions, such as

Alzheimer's.[1] Using the previously shown concept of oppositely charged headgroups being able to induce fusion between two lipid vesicles, a 2-part system comprising vesicles of PA and pHiC was conceptualized. Here the synthesized pHiCL was titrated in order to determine a pK_a. The measured pK_a of the pHiCL will help select a PA with the capacity to lower the localized pH around the pHiCL enough to protonate it, giving rise to the oppositely charged surfaces of lipids ultimately leading to fusion.

The titration of the pHiCL in an aqueous environment gives a uniform titration curve in the forward and reverse directions between alkaline and acidic conditions which is what would be expected. The opposite trend is shown in the titration of pHiCL when combined with a lipid environment in which to anchor itself. The declining fluorescence may be due to the pHiCL burrowing beneath the hydrophobic headgroups after the amine protonation. The lipid used, DLPC, is a possible cause for this burrowing to take place. The net neutral state of DLPC rises from a phosphocholine acting as the hydrophilic headgroup. The phosphocholine contains a primary amine with a positive charge and a phosphate group holding a negative charge. After the pHiCL becomes protonated, the positively charged amine may be pulled toward this phosphate group, effectively closing off the pHiCL from surrounding aqueous environment.

In conclusion, the beginnings of a possible candidate for a pH-inducible cationic lipid to be used for on demand vesicle fusion has been shown. A target localized pH of 6.48 ± 0.02 was determined for the pHiCL in an aqueous environment, but when inserted into a lipid vesicle, the pK_a was inconclusive due to possible interference from the composition of lipid vesicle used. The next step proposed would be to re-titrate the

pHiCL while inserted into lipid vesicles comprising 1,2-dilauroyl-sn-glycerol (12:0 DG). This would remove the possibility of the phosphocholine interference while maintaining a hydrophobic environment for the pHiCL to anchor itself within.

As an alternative change that could be implemented, an electronegative aspect could be applied along the aliphatic tail of the pHiCL. One example being an ester bond linking the hydrophobic tail to the dipicolylamine headgroup of pHiCL could provide enough “buoyancy”. This would possibly repulse the pHiCL headgroup from burying itself into the lipid bilayer due to the negative charge of the phosphocholine headgroup of the DLPC.

Conclusion

This work demonstrates that lipid vesicle fusion has the potential to be combined with other spectroscopic techniques to better understand the vastly unexplored depths of transmembrane protein interactions in their native environment.

Lipid vesicle fusion was achieved without the use of embedded ligands or repeating motifs commonly used to signal or induce fusion. The affinity of an anionic and cationic charged headgroup was able to apply enough strain on the lipid packing to allow for fusion to occur. Fused lipid vesicles were created using both lipid tails of equivalent length (12 carbons) and lipid tails that were different in length by up to two carbons.

A model α-helical peptide, PLA_7, was inserted into an anionic lipid, DLPG. This peptide/lipid system was in turn fused with a cationic lipid, DLEPC, that was 2 carbons longer in length than the DLPG. The difference in length of the fusing lipids caused the PLA_7 to stretch without losing helical secondary structure when the peptide migrated from the shorter DLPG lipid environment to the longer DLEPC environment. This altered structural state was observed using CD spectroscopy and is caused by a weakening of the hydrogen bonding along the backbone of the alpha helix as the amino acids move further apart.

The lipid fusion methods shown are “on-demand” to the degree of mixing the lipids can be controlled but taking it a step further to true on-demand fusion will push the ability to study transmembrane protein interactions to new heights. The outset goal was to use a photoacid and pHiCL with attached aliphatic chains, mimicking lipids, allowing for

them to be inserted into the lipid vesicles altering the surface of the vesicles. A light source of adequate wavelength would deprotonate the photoacid, thus protonating the pHiCL, and establish oppositely charged lipid surface inducing fusion. This method allows for the lipids containing the proteins or contents of interest to reside in the same solution but remain separate until means of observation can be put into place such as CD or dUVRR. The pK_a of the previously described pHiCL was established as 6.48 $\pm$ 0.02 in aqueous solution but could not be determined when inserted into a lipid membrane. This could be caused by the possible burying of the pHiCL into the lipid bilayer due to an attraction between the newly formed cation and the phosphocholine present in headgroup of the DLPC making it impossible to protonate from the surface environment. The proposed solutions take to different paths. The first showing simple switching of the lipid vesicles composition be made of DG (12:0), a similar lipid to the DLPC previously used with a swapping of the phosphocholine for a simple glycerol. The second proposed change comes with the addition of an electronegative element, possibly an ester link, established as a bridge between the pHiCL and attached aliphatic tail. This ester bridge can help resist possible sinking of the pHiCL into the lipid bilayer due to the repulsion between the negative charge of the phosphocholine headgroup and the oxygen of the ester bond.

References

1. Iqbal, K.; Brundke-Iqbal, I.; Wisniewski, H. M., Alzheimer Neurofibrillary Tangle and Its Relationship with Plaque Core Amyloid. In *Amyloidosis*, Glenner, G. G.; Osserman, E. F.; Benditt, E. P.; Calkins, E.; Cohen, A. S.; Zucker-Franklin, D., Eds. Springer US: Boston, MA, 1986; pp 717-722.
2. Sisodia, S. S., Beta-amyloid precursor protein cleavage by a membrane-bound protease. *Proceedings of the National Academy of Sciences of the United States of America* **1992,** *89* (13), 6075-6079.
3. Vassar, R.; Bennett, B. D.; Babu-Khan, S.; Kahn, S.; Mendiaz, E. A.; Denis, P.; Teplow, D. B.; Ross, S.; Amarante, P.; Loeloff, R.; Luo, Y.; Fisher, S.; Fuller, J.; Edenson, S.; Lile, J.; Jarosinski, M. A.; Biere, A. L.; Curran, E.; Burgess, T.; Louis, J. C.; Collins, F.; Treanor, J.; Rogers, G.; Citron, M., Beta-secretase cleavage of Alzheimer's amyloid precursor protein by the transmembrane aspartic protease BACE. *Science* **1999,** *286* (5440), 735-41.
4. Beel, A. J.; Sanders, C. R., Substrate specificity of gamma-secretase and other intramembrane proteases. *Cell Mol Life Sci* **2008,** *65* (9), 1311-34.
5. Pastorino, L.; Lu, K. P., Pathogenic mechanisms in Alzheimer's disease. *European Journal of Pharmacology* **2006,** *545* (1), 29-38.
6. Shimizu, K.; Cao, W.; Saad, G.; Shoji, M.; Terada, T., Comparative analysis of membrane protein structure databases. *Biochimica et Biophysica Acta (BBA) - Biomembranes* **2018,** *1860* (5), 1077-1091.
7. A Liljas, a.; Rossmann, M. G., X-Ray Studies of Protein Interactions. *Annual Review of Biochemistry* **1974,** *43* (1), 475-507.
8. Opella, S. J., Structure determination of membrane proteins by nuclear magnetic resonance spectroscopy. *Annu Rev Anal Chem (Palo Alto Calif)* **2013,** *6*, 305-28.
9. Asamoto, D. K.; Kim, J. E., UV Resonance Raman Spectroscopy as a Tool to Probe Membrane Protein Structure and Dynamics. *Methods Mol Biol* **2019,** *2003*, 327-349.
10. Balakrishnan, G.; Hu, Y.; Nielsen, S. B.; Spiro, T. G., Tunable kHz deep ultraviolet (193-210 nm) laser for Raman application. *Appl Spectrosc* **2005,** *59* (6), 776-81.
11. Halsey, C. M.; Xiong, J.; Oshokoya, O. O.; Johnson, J. A.; Shinde , S.; Beatty, J. T.; Ghirlanda, G.; JiJi, R. D.; Cooley, J. W., Simultaneous Observation of Peptide Backbone Lipid Solvation and α-Helical Structure by Deep-UV Resonance Raman Spectroscopy. *ChemBioChem* **2011,** *12* (14), 2125-2128.
12. Kielian, M., Mechanisms of Virus Membrane Fusion Proteins. *Annual Review of Virology* **2014,** *1* (1), 171-189.
13. Lasic, D. D., The mechanism of vesicle formation. *The Biochemical journal* **1988,** *256* (1), 1-11.
14. Chernomordik, L. V.; Kozlov, M. M., Mechanics of membrane fusion. *Nature Structural & Molecular Biology* **2008,** *15* (7), 675-683.
15. Ma, M.; Gong, Y.; Bong, D., Lipid Membrane Adhesion and Fusion Driven by Designed, Minimally Multivalent Hydrogen-Bonding Lipids. *Journal of the American Chemical Society* **2009,** *131* (46), 16919-16926.

16. Gong, Y.; Ma, M.; Luo, Y.; Bong, D., Functional Determinants of a Synthetic Vesicle Fusion System. *Journal of the American Chemical Society* **2008,** *130* (19), 6196-6205.
17. Ostrowsky, N.; Hesse-Bezot, C., Dynamic light scattering study of the conformational change and fusion phenomenon of phospholipid vesicles. *Chemical Physics Letters* **1977,** *52* (1), 141-144.
18. Hoekstra, D.; Düzgüneş, N., Lipid mixing assays to determine fusion in liposome systems. *Methods Enzymol* **1993,** *220*, 15-32.
19. Düzgüneş, N.; Faneca, H.; de Lima, M. C. P., Methods to Monitor Liposome Fusion, Permeability, and Interaction with Cells. In *Liposomes: Methods and Protocols, Volume 2: Biological Membrane Models*, Weissig, V., Ed. Humana Press: Totowa, NJ, 2010; pp 209-232.
20. Kasha, M., Collisional Perturbation of Spin-Orbital Coupling and the Mechanism of Fluorescence Quenching. A Visual Demonstration of the Perturbation. *The Journal of Chemical Physics* **2004,** *20* (1).
21. Ellens, H.; Bentz, J.; Szoka, F. C., pH-induced destabilization of phosphatidylethanolamine-containing liposomes: role of bilayer contact. *Biochemistry* **1984,** *23* (7), 1532-8.
22. Rouser, G.; Fleischer, S.; Yamamoto, A., Two dimensional thin layer chromatographic separation of polar lipids and determination of phospholipids by phosphorus analysis of spots. *Lipids* **1970,** *5* (5), 494-496.
23. Carpenter, E. P.; Beis, K.; Cameron, A. D.; Iwata, S., Overcoming the challenges of membrane protein crystallography. *Current opinion in structural biology* **2008,** *18* (5), 581-586.
24. Henzler-Wildman, K.; Kern, D., Dynamic personalities of proteins. *Nature* **2007,** *450* (7172), 964-972.
25. Greenfield, N. J., Analysis of Circular Dichroism Data. In *Methods in Enzymology*, Academic Press: 2004; Vol. 383, pp 282-317.
26. Kelly, S. M.; Price, N. C., The use of circular dichroism in the investigation of protein structure and function. *Curr Protein Pept Sci* **2000,** *1* (4), 349-84.
27. Eagleburger, M.; Cooley, J.; Jiji, R., Effects of Fluidity on the Ensemble Structure of a Membrane Embedded alpha-Helical Peptide. *Biopolymers* **2014,** *101*.

VITA

Bryan Matthew Lada was born August 30, 1989 in St.Charles, Missouri. He grew up in St. Louis and Hillsboro, Missouri. In 2007, he graduated from Hillsboro High School. He pursued a Bachelors of Science in Chemistry starting at Jefferson College later transferring to Missouri Baptist University from which he graduated in 2012. Directly after graduating he started in the PhD program at the University of Missouri-Columbia in the lab of Dr. Jason W. Cooley and finishing under Dr. Kent Gates. He will receive his doctorate in chemistry in August 2021.